2018

Boiling Heat Transfer and Pressure Drop of R1234ze(E) inside a Small-Diameter 2.5 mm Microfin Tube

Daisuke Jige
Tokyo University of Marine Science and Technology, Japan, djige00@kaiyodai.ac.jp

Shota Iizuka
Graduate School of Marine Science and Technology, Tokyo University of Marine Science and Technology (2-1-6 Etchujima, Koto-ku, Tokyo, 135-8533, Japan), m164003@edu.kaiyodai.ac.jp

Norihiro Inoue
Tokyo University of Marine Science and Technology, Japan, inoue@kaiyodai.ac.jp

Boiling Heat Transfer and Pressure Drop of R1234ze(E) Inside a Small-Diameter 2.5 mm Microfin Tube

Daisuke JIGE[1]*, Shota IIZUKA[2], Norihiro INOUE[1]

[1]Tokyo University of Marine Science and Technology, Etchujima, Koto-ku, Tokyo, Japan
Phone number: +81-3-5245-7479, Fax number: +81-3-5245-7479
E-mail address: djige00@kaiyodai.ac.jp, inoue@kaiyodai.ac.jp

[2]Graduate School of Marine Science and Technology, Tokyo University of Marine Science and Technology, Etchujima, Koto-ku, Tokyo, Japan

* Corresponding Author

ABSTRACT

This study experimentally investigated the flow boiling heat transfer and pressure drop of R1234ze(E) in a horizontal small-diameter microfin tube with an outer diameter of 2.5 mm and equivalent diameter of 2.1 mm. The boiling heat transfer and pressure drop were measured in the mass velocity range of 100–400 kg/(m^{2}s) and in the heat flux range of 5–20 kW/m^2 at a saturation temperature of 15 °C. The heat transfer coefficient increased as the quality increased because of increasing the forced convection in the pre-dryout region. The heat transfer coefficient increased as the heat flux increased in the low-quality region, but decreased when the heat flux increased past a certain point because the thin liquid film at the fin tips had dried. The heat transfer coefficient increased as the mass velocity increased and exhibited the highest value at a mass velocity of 200 kg/(m^{2}s). The measured heat transfer coefficient agreed well with previous correlations only in the dominant region of the forced convection evaporation. The frictional pressure drop increased as the mass velocity and vapor quality increased, and the measured values agreed well with previously reported correlations for conventional-diameter microfin tubes.

1. INTRODUCTION

The development of high-performance and compact heat exchangers with small-diameter microfin tubes, whose tube diameter is less than 5 mm, is needed to improve the performance of the heat exchanger and reduce the refrigerant charge for air-conditioning systems. The effects of surface tension and shear stress on the boiling heat transfer and flow characteristics become dominant, in comparison to the gravity effect, as the tube diameter decreases. Moreover, the flow boiling characteristics are different from those in conventional-diameter tubes. Many studies have been conducted on boiling heat transfer, pressure drop, and flow characteristics inside conventional-diameter microfin tubes and have clarified these characteristics. Several studies have investigated the boiling heat transfer and pressure drop of small-diameter microfin tubes with an inner diameter of less than 4 mm, in comparison to conventional-diameter microfin tubes. Dang et al. (2010) investigated the boiling heat transfer of CO_2 inside a microfin tube with a mean inner diameter of 2.0 mm, and reported that the heat transfer was significantly affected by heat flux, and that it increased with increasing heat flux because of enhancing the nucleate boiling. Mancin et al. (2015) investigated the boiling heat transfer and pressure drop of R134a inside a microfin tube with a fin-tip diameter of 3.4 mm and reported that the heat transfer was controlled by nucleate boiling and forced convection. Inoue et al. (2016) carried out experiments regarding the boiling heat transfer and pressure drop of R32 inside two microfin tubes with equivalent diameters of 3.5 mm and 3.7 mm and investigated the effect of fin geometry on the flow boiling characteristics. Jige et al. (2016) investigated the boiling heat transfer and pressure drop of R32 inside a microfin tube with an equivalent diameter of 2.6 mm and reported that the tube diameter influenced the boiling heat transfer, and that the heat transfer coefficient in the 2.6 mm microfin tube was 1.3–1.6 times larger in comparison to that of the 3.7 mm microfin tube. Moreover, HFO refrigerants are perceived as refrigerants with a low global warming potential and are expected to replace conventional HFC refrigerants because of worldwide refrigerant regulations. However, few studies have been conducted on the boiling heat transfer and pressure drop of HFO refrigerants in small-diameter microfin tubes with a tube diameter smaller than 5 mm. Diani *et al.* (2014) conducted experiments with R1234ze(E) inside a microfin tube with a fin-tip diameter of 3.4 mm and an outer diameter of 4 mm in the mass velocity range of 190–940 kg/(m^{2}s) and at a saturation temperature of 30 °C. They proposed two prediction correlations for heat transfer and pressure drop in a small-diameter microfin tube. Diani *et al.* (2015) also experimented with R1234yf inside a microfin tube with a fin-tip diameter of 3.4 mm and reported that the heat transfer coefficient increased with increasing heat flux, while the forced convection heat transfer became more effective in the high-quality region. To facilitate the design of evaporators with small-diameter microfin tubes, it is necessary to acquire the measurement data of the boiling heat transfer and pressure drop under a wide range of experimental conditions.

This study experimentally investigated the flow boiling heat transfer and pressure drop characteristics of R1234ze(E) inside a horizontal small-diameter microfin tube with an outer diameter of 2.5 mm and equivalent diameter of 2.1 mm. The experiments were carried out in the mass velocity range of 100–400 kg/(m^{2}s), with a heat flux range of 5–20 kW/m^2, and a saturation temperature of 15 °C. The effects of mass velocity, heat flux, and quality on the flow boiling characteristics were clarified, and the measured heat transfer and pressure drop were compared to previously reported correlations.

2. EXPERIMENTAL APPARATUS AND METHOD

2.1. Experimental Apparatus and Procedure

Figure 1 shows a schematic of the experimental apparatus used in this study. The test apparatus consisted of a pump, water preheater, electric preheater, test section, condenser, receiver, and subcooler. The liquid refrigerant discharged from the gear pump and flowed into the water heat exchanger and electric heater. The electric heater heated the refrigerant to obtain the desired quality at the inlet to the test section. The subcooled liquid refrigerant returned to the pump through the condenser, receiver, and subcooler. The mass flow rate of the refrigerant was measured by a mass flow meter with an accuracy of ±0.5%. The refrigerant flow rate was controlled by the flow control valves in the main and bypass loops.

Figure 2 shows the details of the test section. The test tube was heated by Joule heating with an AC power supply unit. The tube wall temperatures were measured by T-type thermocouples attached onto the test tube wall, separated by 50 mm intervals, and with a measuring accuracy of ±0.05 K. The absolute pressure transducer measured the refrigerant pressure at the inlet of the measuring section with an accuracy of ±1.4 kPa. The pressure drop between the inlet and outlet of the measuring section was measured by differential pressure transducers. The measuring lengths of the heat transfer and pressure drop were 100 and 350 mm, respectively.

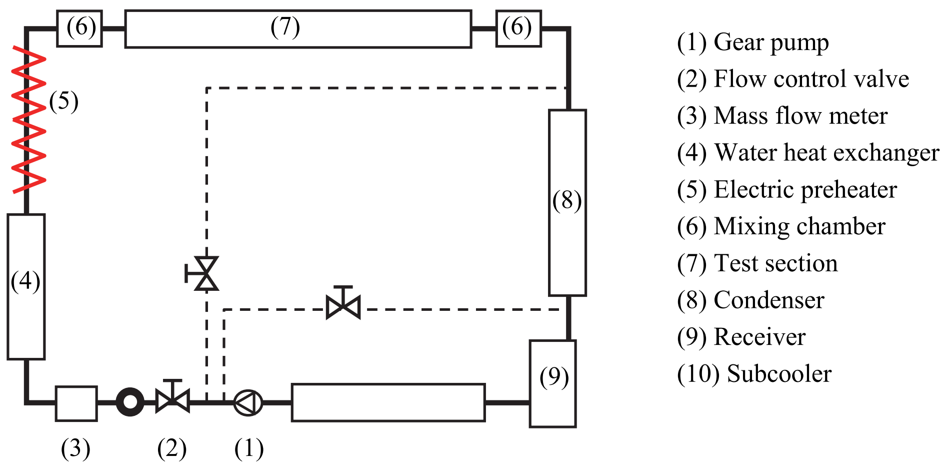

Figure 1: Schematic of experimental apparatus

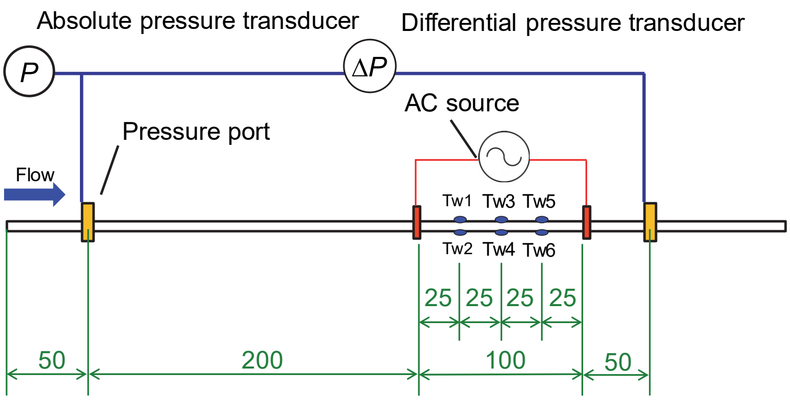

Figure 2: Details of test section

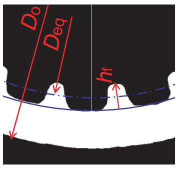

Figure 3: Cross-sectional view of test microfin tube

Table 1: Specifications of test microfin tubes

Outer diameter, D_o [mm]	2.5
Equivalent diameter, D_{eq} [mm]	2.1
Fin height, h_f [mm]	0.1
Number of fins, n_f [-]	25
Helix angle, θ [°]	10
Surface enlargement ratio, η [-]	1.5

Figure 3 shows the cross-sectional view of the test microfin tube. Table 1 gives the specifications of the test microfin tube, which was a small-diameter microfin tube with an outer diameter of 2.5 mm and equivalent diameter of 2.1 mm. The parameters of the test microfin tube were as follows: fin number of 25, helix angle of 10°, fin height of 0.1 mm, and an enlargement surface area of 1.5. The equivalent inner diameter means the inner diameter of a smooth tube with the same internal free flow area as that of the test microfin tube. The enlargement surface area is defined as the ratio of the actual heat transfer area to the surface area of a smooth tube with the same equivalent diameter.

The experiments were carried out using R1234ze(E) as the test refrigerant under a saturation temperature of 15 °C at the inlet to the test section. The heat transfer coefficient and pressure drop were measured in the mass velocity range of 100–400 kg/(m^{2}s) and in the heat flux range of 5–40 kW/m^2.

2.2. Data Reduction

The bulk specific enthalpy at the inlet of the test section ($h_{\mathrm{TS,in}}$) was calculated by the following heat balance equation:

$$h_{\mathrm{TS,in}} = h_{\mathrm{E,in}} + Q_{\mathrm{E}} / m\,, \tag{1}$$

where $h_{\mathrm{E,in}}$ is the specific enthalpy at the inlet of the electric preheater, Q_{E} is the heat transfer rate in the electric preheater, and m is the flow rate of the test refrigerant. The distribution of heat equilibrium quality in the test section was calculated by the distributions of the refrigerant pressure, while the specific enthalpy was calculated by the heat transfer rate in the heating section.

The heat transfer coefficient was calculated by the following equation:

$$\alpha = \frac{Q_{\mathrm{TS}}}{\pi D_{\mathrm{eq}} \eta L (T_{\mathrm{w}} - T_{\mathrm{S}})}\,, \tag{2}$$

where Q_{TS} is the heat transfer rate, D_{eq} is the equivalent inner diameter, L is the effective heating length, η is the surface enlargement ratio calculated by the actual and nominal heat transfer areas, T_w is the inner wall temperature, and T_R is the saturation temperature of the refrigerant. The tube wall temperature is the average temperature of the top and bottom side of the tube. For most of the data, the uncertainty of the boiling heat transfer coefficient calculated based on the calculation procedure given by Jige et al. (2017) was estimated to be within ±10%. The maximum uncertainty was evaluated at 25% with a heat flux of 5 kW/m^2, mass velocity of 200 kg/(m^{2}s), and quality of 0.7.

The frictional pressure drop ΔP_F of the boiling flow was calculated by the following equation:

$$\Delta P_F = \Delta P_{mes} - \Delta P_A \,, \tag{3}$$

where ΔP_{mes} is the measured pressure drop between the inlet and the outlet of the test tube, and ΔP_A is the acceleration pressure drop in the measured section. The acceleration pressure drop was estimated from the following equation.

$$\Delta P_A = \Delta \left(\frac{G^2 x^2}{\xi \rho_V} + \frac{G^2 (1-x)^2}{\xi \rho_L} \right) \tag{4}$$

The void fraction was estimated by the correlation for microfin tube (Kondou *et al.*, 2008). The properties of R1234ze(E) were calculated by NIST REFPROP (Lemmon et al., 2013).

3. EXPERIMENTAL RESULTS

3.1. Boiling Heat Transfer

Figures 4 (a) and (b) show the effect of heat flux on the measured heat transfer coefficient in the microfin tube with an equivalent diameter of 2.6 mm at constant mass velocities of 200 and 400 kg/(m^{2}s). The horizontal and vertical axes represent the quality and heat transfer coefficient, respectively. The heat transfer coefficient of both mass velocities increased with increasing quality because the forced convection heat transfer was enhanced under any heat flux condition. In particular, at a mass velocity of 200 kg/(m^{2}s) and heat flux of 5 kW/m^2, the heat transfer coefficient increased rapidly as the quality increased at x=0.3. For microfin tubes, the heat transfer was enhanced by the extremely thin liquid film that was formed in the grooves; namely, the meniscus liquid film. It is thought that

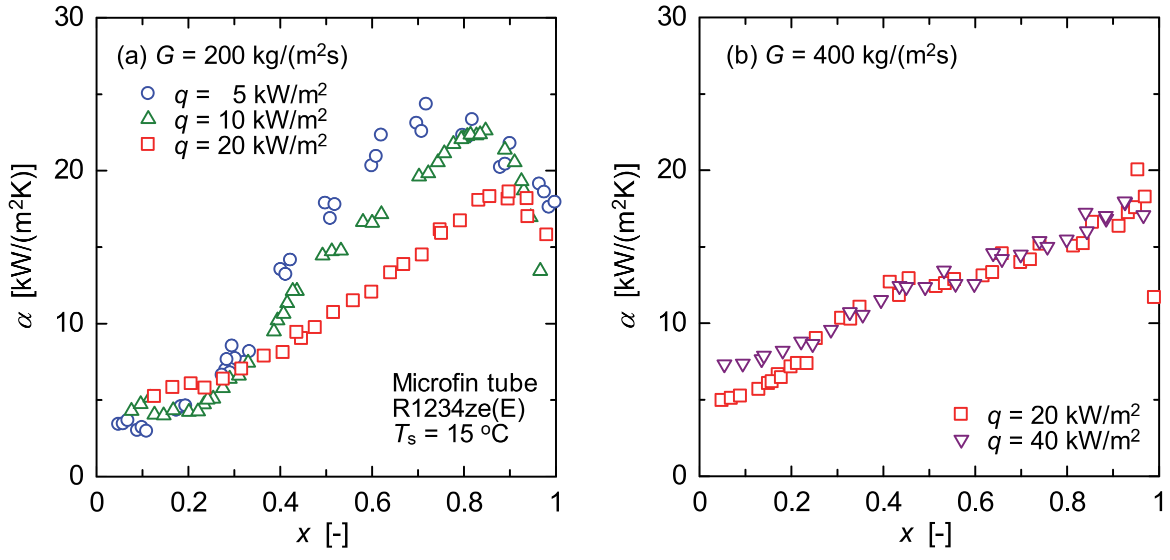

Figure 4: Effect of heat flux on heat transfer coefficient at mass velocities of 200 and 400 kg/(m^{2}s).

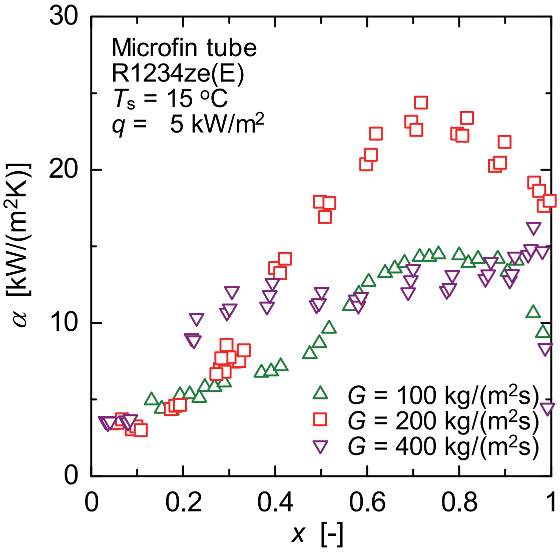

Figure 5: Effect of mass velocity on heat transfer coefficient at heat flux of 5 kW/m^2

this heat transfer enhancement was caused by the flow pattern transitioning to annular flow with a liquid meniscus film. The heat transfer coefficient of both mass velocities increased as the heat flux increased with a quality less than 0.3, because of enhanced nucleate boiling. In contrast, the mass velocity heat transfer coefficient of 200 kg/(m^{2}s) decreased as the heat flux increased in the higher quality region. It is thought that the liquid film thickness decreased as the quality increased, and that the liquid film at the fin tips dried because of the heat flux increasing. However, the effect of the heat flux on the heat transfer coefficient was small at G = 400 kg/(m^{2}s) and with higher quality. At the mass velocity of 400 kg/(m^{2}s) in the higher-quality region, the flow pattern estimated the annular flow with a uniform liquid film thickness, and the liquid film flowed across the microfins. Therefore, the deterioration of the heat transfer because of the dryness at the fin tips was suppressed because a liquid meniscus did not exist. Similar trends, which were the effects of the quality and heat flux on the heat transfer characteristics, have been reported by a previous study using R32 as the test refrigerant inside a microfin tube with an equivalent diameter of 2.6 mm (Jige et al., 2016).

Figure 5 shows the effect of mass velocity on the heat transfer coefficient at a heat flux of 5 kW/m^2. The effect of the mass velocity on heat transfer was small with a quality of less than 0.2. The heat transfer coefficient for the mass velocities of 100, 200, and 400 kg/(m^{2}s) increased dramatically as the quality increased at x = 0.5, 0.3, and 0.1, respectively. This heat transfer enhancement was caused by the flow pattern that transitioning to annular flow with a liquid meniscus in the grooves. The heat transfer coefficient increased as the mass velocity increased, under 200 kg/(m^{2}s), because of increasing the vapor shear stress, but it decreased with the further increase of the mass velocity because the circumferential liquid film thickness became uniform and the liquid flowed across the microfins. Therefore, the highest value of the heat transfer coefficient was observed at G = 200 kg/(m^{2}s) in a higher quality region.

Figures 6 (a) and (b) show the heat transfer coefficient differs at the top and bottom sides of the microfin tube at the mass velocities of 100 and 400 kg/(m^{2}s). For a mass velocity of 400 kg/(m^{2}s), there was no difference in the heat transfer coefficients at the top and bottom sides of the tube. Therefore, it was thought that the flow pattern was the annular flow and that the circumferential liquid film thickness was uniform. Moreover, for a mass velocity of 100 kg/(m^{2}s), the heat transfer coefficient at the top side of the tube indicated a higher value, in comparison to the bottom side in the lower quality region. This difference in the heat transfer coefficient suggested that the liquid film thickness at the bottom side was thick, in comparison to the upper side, owing to the effect of gravity. Additionally, the influence of gravity could be confirmed even in a 2.1 mm microfin tube with lower mass velocity and quality. However, the influence of gravity was not observed at a higher vapor velocity.

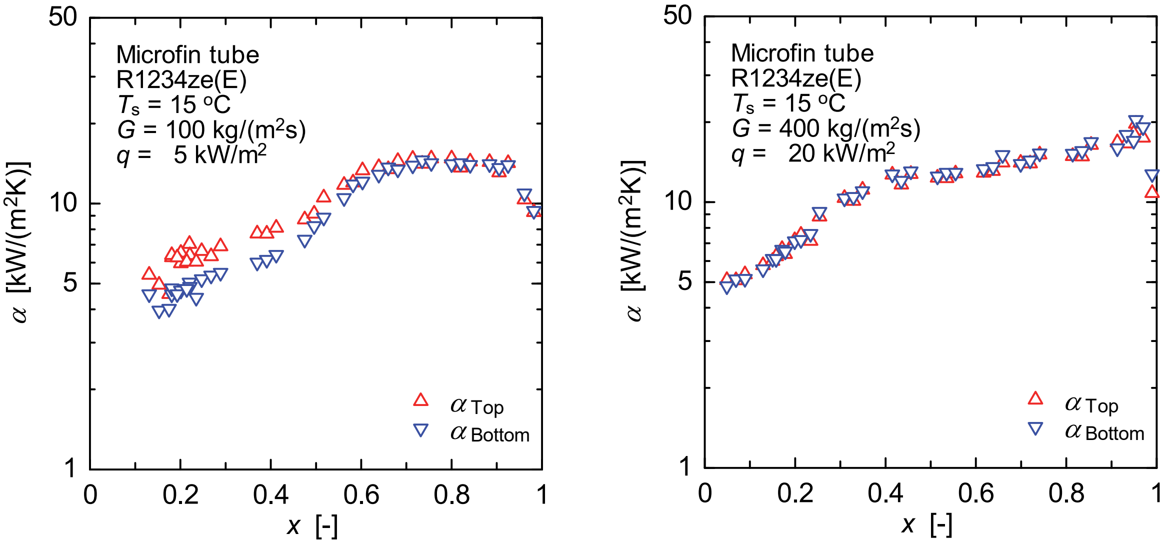

Figure 6: Difference of heat transfer coefficient between top and bottom sides of microfin tube at mass velocities of 100 and 400 kg/(m^{2}s)

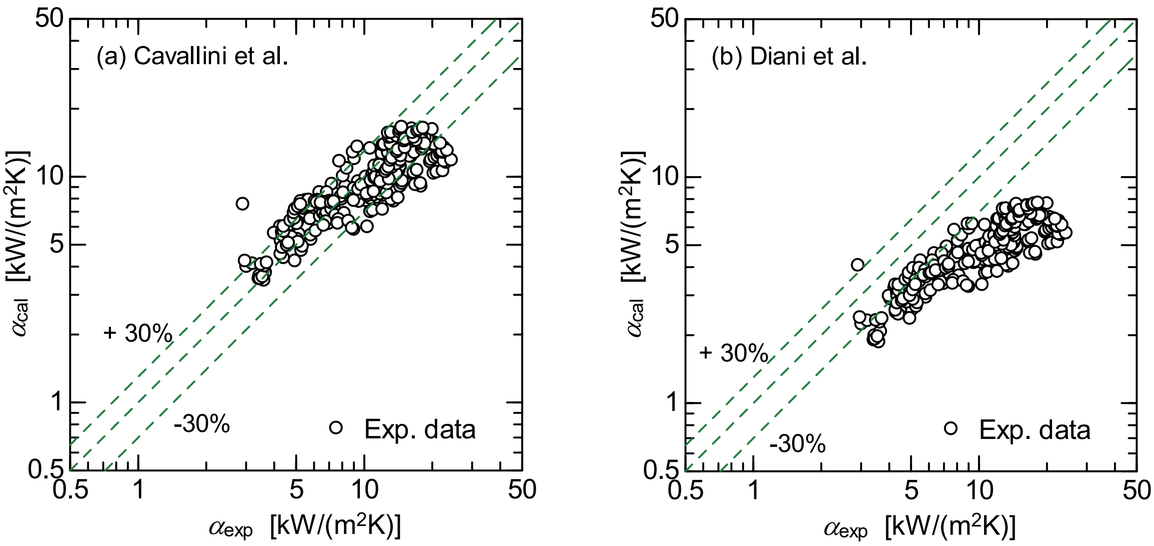

Figure 7: Comparison between measured heat transfer coefficient and predicted values calculated by correlations (Cavallini et al., 1999: Diani et al., 2014)

Figures 7 (a) and (b) show a comparison between the measured heat transfer coefficient and the predicted values calculated using the correlations for the microfin tubes (Cavallini et al., 1999, Diani et al., 2014). The correlation of Diani et al., which was proposed for a small-diameter microfin tube, slightly underpredicted the data obtained in this study. However, the correlation of Cavallini et al., which was proposed for conventional-diameter microfin tubes, was in good agreement with the data obtained in this study inside the 2.1 mm microfin tube.

3.2. Frictional Pressure Drop

Figure 8 shows the frictional pressure drop inside the microfin tube with a 2.1 mm equivalent diameter on the boiling flow and within the heat flux range of 5–10 kW/m^2. In this comparison, the quality change in the measured section was within 0.05. The measured frictional pressure drop increased with increasing quality and mass velocity because of increasing the vapor shear stress. The frictional pressure drop at a mass velocity of 400 kg/(m^{2}s) was four times that of G = 200 kg/(m^{2}s) with the same quality. The measured frictional pressure drop was compared to the correlations of Filho et al. (2004) regarding conventional-diameter microfin tubes, and to those of Diani et al. (2014)

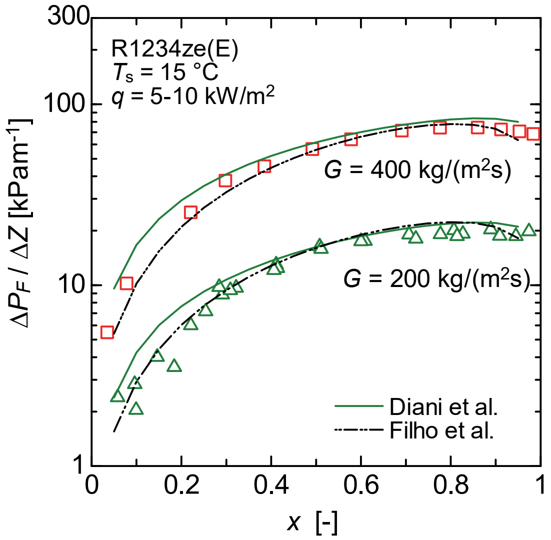

Figure 8: Frictional pressure drop at mass velocities of 200 and 400 kg/(m^{2}s)

regarding small-diameter microfin tubes, as shown in Figure 8. The Diani et al. correlation agreed well with the data obtained in this study in the higher quality region, but slightly overpredicted the results obtained in the low-quality region. The Filho et al. correlation was proposed based on the data of a microfin tube with an inner diameter of 6.4–8.9 mm and using R134a. This correlation agreed well with the measured pressure drop of R1234ze(E) inside the 2.1 mm microfin tube.

4. CONCLUSIONS

This study experimentally investigated the boiling heat transfer and pressure drop characteristics of R1234ze(E) inside a horizontal small-diameter microfin tube with an equivalent diameter of 2.1 mm and outer diameter of 2.5 mm. The main conclusions drawn from this investigation are summarized as follows:

(1) The heat transfer coefficient increased with increasing heat flux in the low-quality region because of the enhanced nucleate boiling. However, it decreased as the heat flux increased at a lower mass velocity and in a higher quality region because the thin liquid film at the fin tips had dried. This dryness at the fin tips was suppressed by increasing the mass velocity.

(2) The heat transfer coefficient increased rapidly as the quality increased at certain quality values, as a result of the flow pattern transitioning to annular flow with a meniscus. This flow pattern transition could be confirmed based on the measured heat transfer coefficients at the top and bottom sides of the tube.

(3) The heat transfer coefficient increased with the mass velocity under a mass velocity of 200 kg/(m^{2}s), while it decreased as the mass velocity increased further because the circumferential liquid film thickness became uniform and the liquid flowed across the microfins as the vapor shear stress increased.

(4) The correlation of Cavallini et al. (1999) for conventional-diameter microfin tubes agreed well with the present data of the heat transfer coefficient inside the 2.1 mm microfin tube.

(5) The measured frictional pressure drop increased with the quality and mass velocity because of increasing the vapor shear stress. The data obtained in this study were predicted using the frictional pressure drop correlation of Filho *et al.* (2004).

NOMENCLATURE

D	diameter	(m)
G	mass velocity	(kg/(m^{2}s))
h_f	fin height	(m)
h	specific enthalpy	(J/kg)
L	heat transfer length	(m)
n	Number of fins	(-)

q	heat flux	(W/m^2)
Q	heat transfer rate	(W)
T	temperature	(K)
T_s	saturation temperature	(K)
x	vapor quality	(-)
α	heat transfer coefficient	(W/(m^{2}K))
$\Delta P/ \Delta Z$	pressure drop gradient	(Pa/m)
η	surface enlargement ratio	(-)
θ	helix angle	(°)

Subscripts

A	acceleration
Bottom	bottom side
cal	calculation value
E	pre-heater
eq	equivalent
exp	experimental value
f	fin
F	friction
in	inlet
mes	measured
Top	top side
TS	test section
w	tube wall

REFERENCES

Cavallini A, Del Col D, Doretti L, Longo GA, Rossetto L. 1999, Refrigerant vaporization inside enhanced tubes: a heat transfer model. Heat Technology. 17, 29–36.

Dang C, Haraguchi N, Hihara E. 2010, Flow boiling heat transfer of carbon dioxide inside a small-sized microfin tube. Int. J. Refrigeration, 33, 655–663.

Diani A, Mancin S, Rossetto L. 2014, R1234ze (E) flow boiling inside a 3.4 mm ID microfin tube, Int. J. Refrig. 47:105–119.

Diani A, Mancin S, Rossetto L. 2015, Flow boiling heat transfer of R1234yf inside a 3.4 mm ID microfin tube, Experimental Thermal and Fluid Science.66:127-136.

Filho EPB, Jabardo JMS, Barbieri PEL. 2004, Convective boiling pressure drop of refrigerant R-134a in horizontal smooth and microfin tubes, Int. J. Refrig. 27: 895–903.

Inoue N, Jige D, Sagawa K. 2016, Evaporation heat transfer and pressure drop of R32 inside small-diameter 4.0 mm tubes, International Refrigeration and Air Conditioning Conference, Paper 2394.

Jige D, Sagawa K, Inoue N. 2016, Flow boiling heat transfer characteristics of R32 inside a horizontal small-diameter microfin tube, International Refrigeration and Air Conditioning Conference, Paper 2371.

Jige, D., Sagawa, K., Inoue, N., 2017, Effect of tube diameter on boiling heat transfer and flow characteristic of refrigerant R32 in horizontal small-diameter tubes, Int. J. Refrig. 76: 206–218.

Kondou C, Kuwahara K, Koyama S, 2008, An experimental study on void fraction of CO_2 flow boiling in a horizontal micro-fin tube, International Refrigeration and Air Conditioning Conference, Paper 985.

Lemmon EW, Huber ML, McLinden MO. 2013, Reference Fluid Thermodynamic and Transport Properties-REFPROP, Version 9.1, National Institute of Standards and Technology (NIST), Standard Reference Data Program, Gaithersburg.

Mancin S, Diani A, Rossetto L. 2015, Experimental measurements of R134a flow boiling inside a 3.4 mm ID microfin tube. Heat Transf. Eng., 36, 1218–1229.

ACKNOWLEDGEMENT

We would like to express our gratitude to the Japan Copper Development Association for partially supporting this study.